Research Square

Preprints are preliminary reports that have not undergone peer review.
They should not be considered conclusive, used to inform clinical practice,
or referenced by the media as validated information.

Exosomes From LPS-stimulated hDPSCs Promote the Angiogenesis of HUVECs

Xiangyu Huang
Department of Stomatology, Nanfang Hospital, Southern Medical University, School of Stomatology
Wei Qiu
Department of Stomatology, Nanfang Hospital, Southern Medical University, School of Stomatology
Yuhua Pan
Department of Stomatology, Nanfang Hospital, Southern Medical University, School of Stomatology
Jianjia Li
Department of Stomatology, Nanfang Hospital, Southern Medical University, School of Stomatology
Zhao Chen
Department of Stomatology, Nanfang Hospital, Southern Medical University, School of Stomatology
Kaiying Zhang
Department of Stomatology, Nanfang Hospital, Southern Medical University, School of Stomatology
Yifei Luo
Department of Stomatology, Nanfang Hospital, Southern Medical University, School of Stomatology
Buling Wu
Department of Stomatology, Nanfang Hospital, Southern Medical University, School of Stomatology; Shenzhen Stomatology Hospital (Pingshan), Southern Medical University
Wenan Xv (venus_200@163.com)
Department of Stomatology, Nanfang Hospital, Southern Medical University, School of Stomatology, 1838 Guangzhou Avenue North, Guangzhou 510515, China https://orcid.org/0000-0002-7481-5283

Research

Keywords: Inflammation, Dental pulp stem cells, Exosomes, Angiogenesis, microRNA

Posted Date: November 2nd, 2020

DOI: https://doi.org/10.21203/rs.3.rs-99756/v1

License: This work is licensed under a Creative Commons Attribution 4.0 International License.
Read Full License

Abstract

Background: Angiogenesis is fundamental to biomimetic pulp regeneration. Extracellular vesicles (EVs) derived from human dental pulp stem cells (hDPSCs) from patients with periodontitis were reported to have better angiogenic capabilities. However, the underlying regulatory mechanism remains unknown. As an important component of EVs, exosomes from hDPSCs were indicated to play a crucial role in multiple regeneration processes. In this study, the inflammatory factor lipopolysaccharide (LPS) was used to stimulate hDPSCs, and exosomes were extracted from these hDPSCs. The role of exosomes in the angiogenesis of Human Umbilical Vein Endothelial Cells (HUVECs) was examined, and the underlying mechanism was studied.

Method: Exosomes were isolated from hDPSCs with or without LPS stimulation. The angiogenic capabilities of HUVECs were evaluated after coculture with exosomes derived from hDPSCs (hDPSC-EXOs) or exosomes derived from LPS-stimulated hDPSCs (LPS-hDPSC-EXOs). Tube formation and migration assays were conducted, and angiogenesis-related mRNA expression was detected. MicroRNA sequencing was performed to explore the microRNA profile of hDPSC-EXOs and LPS-hDPSC-EXOs. Gene Ontology (GO) analysis was used to study the functions of the predicted target genes. Kyoto Encyclopedia of Genes and Genomes (KEGG) pathway analysis was used to estimate the signaling pathways associated with the inflammation-induced angiogenesis process.

Result: The release of hDPSC-EXOs increased after stimulation with LPS. Compared to endocytosis of hDPSC-EXOs, endocytosis of LPS-hDPSC-EXOs promoted the tube formation and migration of HUVECs. The mRNA expression levels of vascular endothelial growth factor (VEGF) and kinase-insert domain-containing receptor (KDR) in the LPS-hDPSC-EXOs group were significantly higher than those in the hDPSC-EXOs group. MicroRNA sequencing showed that 10 microRNAs were significantly changed in LPS-hDPSC-EXOs; of these microRNAs, 7 were increased, and 3 were decreased. Pathway analysis showed that the genes targeted by differentially expressed microRNAs were involved in multiple angiogenesis-related pathways.

Conclusion: This study revealed that exosomes derived from inflammatory hDPSCs displayed a stronger effect on vascular regeneration. It’s the first time to explore the role of exosomal microRNA from hDPSCs in inflammation-induced angiogenesis. This finding sheds new light on the effect of inflammation-stimulated hDPSCs on tissue regeneration.

Introduction

Stem cell-based dental pulp regeneration has been considered a novel approach for the treatment of inflamed pulp tissue. However, revascularization in pulpal tissue remains the greatest challenge in biomimetic pulp regeneration. As vascular system reconstruction is a prerequisite for nutrient and oxygen transportation, angiogenesis plays a fundamental role in pulp regeneration.

hDPSCs are a type of mesenchymal stem cell (MSC) with excellent pluripotency and proliferation potential. hDPSCs can be separated conveniently and noninvasively from extracted teeth. Located in a neurovascular niche, hDPSCs have strong potential for neurogenesis and angiogenesis[1]. Many studies have shown that hDPSCs perform their proangiogenic function by guiding endothelial cells[2]. The conditioned medium, secretome, and cytokines from hDPSCs were proven to promote endothelial cell migration and tubulogenesis, and these findings indicated the importance of the paracrine mechanism in the revascularization process[3–5]. In response to inflammatory stimulation, immunoregulation and regenerative events could be induced by hDPSCs. In these cases, hDPSCs show great clinical value in dental pulp repair and regeneration.

hDPSCs exhibit strong regeneration potential in controlled inflammatory microenvironments, and this potential includes strong differentiation potency and great cellular proliferation, migration, and homing abilities[6]. A similar phenomenon was observed in terms of angiogenesis. Increased blood vessel density was observed in pulpal tissues from deep caries and pulpitis [7]. In response to stimulation with lipopolysaccharides (LPS), vascular endothelial growth factor (VEGF) expression could be induced in hDPSCs via mitogen-activated protein kinase (MAPK) signaling[8]. However, the mechanism of the proangiogenic effects of inflammatory hDPSCs remains unclear.

Exosomes, a crucial element in paracrine mechanisms, are an important means of intercellular communication[9]. As a type of extracellular vesicles (EVs) with a diameter of 30–150 nm, exosomes display favorable safety and stability. Exosomes can migrate in certain directions. The complex cargo contained in exosomes can reflect the state of the parental cells[10]. All these advantages make exosomes a promising cell-free therapeutic tool for regeneration. MSC-derived exosomes display regulatory functions via mRNA, microRNA, and protein transfer[11]. It has been proven that the angiogenesis of target cells can be regulated by microRNAs from exosomes[12]. Xian et al. showed that exosomes from dental pulp cells could promote the proliferation, cytokine expression, and tube formation of human umbilical vein endothelial cells (HUVECs) via p38 MAPK signaling[5]. Interestingly, EVs secreted by inflammatory hDPSCs showed superior abilities in new vessel formation and cutaneous wound healing compared to EVs secreted by healthy teeth. Taken together, these results raised the question of whether exosomes from inflammatory hDPSCs contribute to improved angiogenic abilities[13]. In this study, we hypothesized that exosomes derived from hDPSCs from the inflammatory environment have stronger proangiogenesis effects, and these properties are mediated by specific exosomal microRNAs.

In this study, exosomes derived from LPS-stimulated hDPSCs were isolated and characterized. The angiogenic abilities of the exosomes was studied. In addition, microRNA expression profiles of LPS-stimulated hDPSC-derived exosomes were analyzed to elucidate the role of microRNAs and the underlying mechanism. To the best of our knowledge, this is the first study to reveal that exosomal microRNAs from inflammatory hDPSCs can promote the angiogenesis of HUVECs.

Materials And Methods

1. hDPSC isolation, culture, and identification

Third molars without periodontitis or caries from healthy human donors (aged 18–24 years) were extracted and collected at the Department of Oral and Maxillofacial Surgery, Nanfang Hospital, Guangzhou, China. This study was approved by the Ethics Committee of Nanfang Hospital, Southern Medical University. Informed consent was obtained from each patient. Pulp tissues were digested to isolate hDPSCs[14, 15]. Subsequently, the hDPSCs were cultured in Dulbecco's modified Eagle's medium (DMEM; Gibco, Grand Island, NY, USA) supplemented with 10% fetal bovine serum (FBS; Gibco, Grand Island, NY, USA), 100 U/mL penicillin, and 100 mg/mL streptomycin (HyClone, NY, USA), in a 5% CO_2 atmosphere at 37 °C. Flow cytometry (Becton Dickinson, Tokyo, Japan) was conducted to identify stem cell surface markers. Passage 3 hDPSCs were suspended at a final density of 5×10^5 cells/ml and incubated with conjugated human antibodies, including CD29-PE, CD90-PE, CD34-PE, CD45-FITC, CD44-FITC, and CD90-FICT (BD Pharmingen, Franklin Lakes, NJ) in the dark for 1 hour at 4 °C. After washing with phosphate-buffered saline (PBS; Corning, NY, USA), the cells were subjected to flow cytometric analysis.

2. Multilineage differentiation assay

Osteogenic and adipogenic induction were performed to determine the multilineage differentiation potential of the hDPSCs. Passage 3 hDPSCs were cultured in 6-well plates for 14 days. In the osteogenic induction group, 100 nM dexamethasone, 10 mmol/L β-glycerophosphate, and 50 mg/mL ascorbic acid (Sigma, St Louis, MO, USA) were added to the culture medium, and the mineralized nodules were stained with 2% Alizarin red S (Alizarin Red S A5533, Sigma-Aldrich). In the adipogenic differentiation group, 1 mmol/L dexamethasone, 0.05 mmol/L methyl isobutyl xanthine, 10 mg/mL insulin, and 200 mmol/L indomethacin (Sigma, St Louis, MO, USA), were added to the culture medium, and the lipid droplets were visualized by oil red O staining following a standard protocol.

3. cell viability assay

The hDPSCs were seeded in 96-well plates at a density of 2×10^3 cells/well and were stimulated with different concentrations of LPS (Sorlarbio, Beijing, China; 0, 1, 5, 10 and 50 μg/mL) for 2 days. Ten microliters of Cell counting kit-8 reagent (CCK-8; Beyotime Biotechnology, Shanghai, China) was added to each well. After 2 hours of incubation in the dark, the absorbance was measured at a wavelength of 490 nm using a microplate reader (BioTEK, Swindon, UK). Triplicate repeats were used in this assay.

4. Exosome-free serum preparation and exosome collection

Fetal bovine serum was diluted in DMEM to 20%. Overnight ultracentrifugation at 100,000 g was performed to eliminate the serum-derived exosomes[16]. After reaching 70% confluence, hDPSCs (passages 3 to 5) were cultured in DMEM containing 10% exosome-free bovine serum and 1% penicillin-streptomycin with or without 5 μg/mL LPS for 2 days. The culture medium was collected for exosome purification by programmed centrifugation. The culture medium was centrifuged at 300 × g for 10 min, and the supernatant was harvested for another centrifugation at 2,000 × g for 10 min. To remove the

extracellular vesicles and apoptotic bodies, the supernatants from the previous step were collected and centrifuged at 10,000 × g for 30 min. To purify the exosomes, the supernatants were ultracentrifuged (Optima XPN-100, Beckman Coulter, USA) at 100,000 × g for 70 min. The sedimentary pellet was resuspended in phosphate-buffered saline (PBS) and then ultracentrifuged at 100,000 × g for another 70 min. The exosome pellet was resuspended in 20 μL PBS and stored at -80°C.

5. Exosome identification and BCA protein assay

The protein concentration of the exosomes was quantified with a micro BCA Protein Assay Kit (Thermo Fisher, USA). Transmission electron microscopy (TEM) was used to identify the exosome morphology. The exosomes were pipetted onto formvar/carbon-coated TEM grids at room temperature. After staining with 4% uranyl acetate, images of the exosomes were captured by TEM (JEM-1400 PLUS,Tokyo, JAPAN). The particle diameter was determined by Nanoparticle Tracking assay (NTA) with a Nanosight NS300 (Malvern, Worcestershire, UK). The exosomal surface markers CD9, CD63 and heat shock protein 70 (HSP70; System Biosciences, PA, USA) were examined using automated Western blotting.

6. Exosome endocytosis assay

PKH67 (0.4 μL, Sigma-Aldrich, St Louis, MO) was added to 200 μL Diluent C and incubated with 20 μL exosomes for 2 min at room temperature. Then, 200 μL exosome-free FBS was added to terminate the reaction. The exosomes were washed in PBS and ultracentrifuged at 100,000 × g for 70 min. HUVECs were cultured in an endothelial growth medium-2 bullet kit (EGM-2; Lonza CC-3162, MD, USA) at 37 °C with 5% CO2. PKH67-labeled exosomes were added and incubated for 4 hours at 37 °C. The HUVECs were fixed with 4% paraformaldehyde for 20 min. Antifade Mounting Medium with 4',6-diamidino-2-phenylindole (DAPI; Beyotime Biotechnology, Shanghai, China) was used for nuclear staining. The images of exosome endocytosis by HUVECs were captured with an electric inverted microscope (Olympus, Tokyo, Japan).

7. Tube formation assay for angiogenesis

HUVECs were pretreated with exosomes derived from hDPSCs (hDPSC-EXOs) or exosomes derived from LPS-stimulated hDPSCs (LPS-hDPSC-EXOs) (100 μg/mL) for 24 hours. An equal volume of PBS was added to the control group. HUVECs were resuspended, seeded onto Matrigel (150 μL) (BD Biosciences, San Jose, CA)-precoated 48-well plates at a density of 10^5 cells/well, and incubated at 37 °C for 1 to 9 hours. Exosomes or PBS was added to each well. Images of tube formation were obtained with microscope. The indexes of tube formation were analyzed by ImageJ software.

8. Migration assay

A scratch wound healing assay was used to estimate the migration ability of HUVECs in response to hDPSC-EXOs or LPS-hDPSC-EXOs. HUVECs were seeded in 12-well plates at a density of 1×10^5 cells/well. After reaching 80% confluence, a scratch was made with a sterile pipette tip in each well. After washing with PBS, the HUVECs were exposed to fresh culture medium with hDPSC-EXOs or LPS-hDPSC-

EXOs (100 μg/mL). An equal volume of PBS was added to the control group. Images of scratches were captured at 0 hours, 12 hours, and 24 hours.

9. MicroRNA sequencing

A total of 3 μg RNA was extracted from each exosome sample and sent to Novogene Co., Ltd. (Beijing, China) for the construction of a small RNA library. After cluster generation, the libraries were sequenced on an Illumina HiSeq 2500 platform (Illumina, CA, USA), and 50-bp single-end reads were generated. A *P*-value of 0.05 was set as the threshold for significant differential expression by default. Differentially expressed microRNAs were analyzed. The microRNA target genes were predicted by two bioinformatics tools (miRanda and RNAhybrid). Gene Ontology (GO; http://geneontology.org/) enrichment analysis was used to define gene attributes in organisms from three fields: biological processes (BP), cellular components (CC), and molecular functions (MF). ($P < 0.05$ was used). KOBAS software was used to test the statistical enrichment of the target gene candidates in the Kyoto Encyclopedia of Genes and Genomes (KEGG) pathway database (KEGG; https://www.genome.jp/kegg/pathway.html)

10. Quantitative reverse-transcription polymerase chain reaction (qRT-PCR)

mRNA and microRNA were extracted from cells or exosomes by the RNA Isolater Total RNA Extraction Reagent (Vazyme Biotech Co., Ltd, Nanjing, China). Total RNA was reverse transcribed into cDNA using a HiScript II 1st Strand cDNA Synthesis Kit (Vazyme Biotech Co., Ltd, Nanjing, China) or a miDETECT A Track miRNA qRT-PCR Starter Kit (RiboBio Ltd., Guangzhou, China). qRT-PCR was performed by the SYBR-Green PCR kit (Vazyme Biotech Co., Ltd, Nanjing, China) according to the manufacturer's instructions on a QuantStudio5 system (Thermo Fisher Scientific, Waltham, MA, USA). U6 and glyceraldehyde-3-phosphate dehydrogenase (GAPDH) were used as the internal controls for microRNA and mRNA, respectively. The primers for miRNAs were designed by RiboBio Corporation (Guangzhou, China). The sequences of the mRNA primers are listed below. VEGF: forward, 5'-gggcagaatcatcacgaagt-3', and reverse 5'-tggtgatgttggactcctca-3'. Kinase-insert domain-containing receptor (KDR): forward, 5'-gtgaccaacatggagtcgtg-3', and reverse 5'-tgcttcacagaagaccatgc-3'. Angiopoietin 1 (Ang-1): forward, 5'-gaagggaaccgagcctattc-3', and reverse 5'-gggcacatttgcacatacag-3'. Thrombospondin 1 (THBS): forward, 5'-aggcatgttccagtttcacc-3', and reverse 5'-gctggcaccacctttattgt-3'. Interleukin-6 (IL-6): forward, 5'-aggagacttgcctggtgaaa-3', and reverse 5'-caggggtggttattgcatct-3'. Tumor necrosis factor alpha (TNF-α): forward, 5'-ctatctgggaggggtcttcc-3', and reverse 5'-ggttgagggtgtctgaagga-3'. Glyceraldehyde-3-phosphate dehydrogenase (GAPDH): forward, 5'-cgaccactttgtcaagctca-3', and reverse 5'-aggggtctacatggcaactg-3'.

11. Statistical analysis

Each experiment was repeated in triplicate. All the values are presented as the mean ± SD and were analyzed in SPSS 19.0 (SPSS Inc., USA). A paired *t*-test was used for two-group comparisons. One-way analysis of variance (ANOVA) followed by Dunnett's T3 was used for multiple group comparisons. $p < 0.05$ was regarded as statistically significant.

Results

1. Isolation and characterization of hDPSCs

The hDPSCs were extracted from healthy human third molars. The primary cultured dental pulp stem cells grew around the tissue mass (Fig. 1A). Morphological observation showed cells with fibroblast-like appearances (Fig. 1B). The Alizarin red staining and oil red O staining results showed that the hDPSCs could be differentiated into osteoblasts and adipocytes, respectively (Fig. 1C, D), indicating the multilineage differentiation potential of hDPSCs. The surface markers of the cells were detected by flow cytometry. The results reflected that the hDPSCs expressed high levels of the mesenchymal stem cell markers CD90 (90.5%), CD44 (99.27%), and CD29 (99.63%) and expressed minimal levels of the hematopoietic cell markers CD45 (0.16%), CD34 (0.32%), and CD105 (3.49%), indicating the mesenchymal lineage of hDPSCs (Fig. 1E-J).

2. **Characterization of exosomes from LPS-stimulated hDPSCs.**

hDPSCs were stimulated with different concentrations of LPS (0, 1, 5, 10 or 50 μg/mL). The CCK-8 assay showed the effect of LPS on hDPSC viability. No significant difference was observed between the 0, 1 and 5 μg/mL groups. However, compared to that in the control group, the cell viability in the 10 and 50 μg/mL groups was decreased to 70% and 62%, respectively (Fig. 2A). The IL-6 and TNF-α expression levels were used as indicators in the in vitro inflammation model. After stimulation with LPS for 24 hours, the IL-6 and TNF-α expression levels in the hDPSCs were obviously increased in a dose-dependent manner ($P < 0.05$) (Fig. 2B). LPS (5 μg/ml) was used as the optimal concentration for stimulation, since this concentration could induce an inflammatory microenvironment without reducing cell viability.

Exosomes from hDPSCs were treated with or without LPS stimulation for 2 days and were harvested by programmed ultracentrifugation. TEM was used to detect the shapes of the exosomes. The extracellular vesicles from the hDPSCs presented a typical exosome shape, that is, they were round cup-shaped with a bilayer membrane (Fig. 2C). To accurately measure the different particle sizes, NTA was used. Most of the exosome diameters ranged from 30 to 150 nm, which was consistent with the standard size of exosomes (Fig. 2D). Finally, exosome-specific markers (CD9, CD63, and HSP70) were detected by Western blotting (Fig. 2E). These results indicated that the main content of the purified extracellular vesicles was exosomes.

The BCA assay results showed that the hDPSCs in the LPS-induced inflammatory microenvironment produced more exosomes than those in the normal microenvironment. Furthermore, there was a positive correlation between LPS concentration and exosome volume. The exosome production from 5 μg/mL LPS-treated hDPSCs was higher than that from 1 μg/mL LPS-treated hDPSCs (Fig. 2F).

3. Exosomes derived from LPS-stimulated hDPSCs promoted the angiogenesis and migration of HUVECs

The hDPSC-EXOs and LPS-hDPSC-EXOs labeled with PKH-67 were taken up by HUVECs and were mainly located in the cytoplasm (Fig. 3A). This result indicated that exosomes could be a vehicle for intercellular communication.

A scratch wound healing assay was used to evaluate the effect of LPS-hDPSC-EXOs on the migration capability of HUVECs. At 12 hours, the HUVECs in the LPS-hDPSC-EXOs group exhibited significantly increased motility compared to the HUVECs in the hDPSC-EXOs group and control group. At 24 hours, the boundaries of the scratches in both the hDPSC-EXOs group and LPS-hDPSC-EXOs group were remarkably smaller than those in the control group (Fig. 3B). The results above showed that the HUVECs in the LPS-hDPSC-EXOs group exhibited a stronger migration ability than those in the hDPSC-EXOs group.

To investigate the different angiogenic effects of hDPSC-EXOs and LPS-hDPSC-EXOs, HUVECs were seeded on Matrigel-coated 96-well plates. After treatment with 100 μg/mL hDPSC-EXOs or LPS-hDPSC-EXOs for 1 hours and 9 hours, the number of junction points and total tube length were analyzed. At the early stage of angiogenesis (1 hours), capillary-like structures begin to form. The chains-structures could be observed in all the groups. The total tube length and junction points were higher in the LPS-hDPSC-EXOs group than those in hDPSC-EXOs group. ($P < 0.05$; Fig. 4A-C). At 9 hours, the late stage of angiogenesis, endothelial vessel-like networks had formed in hDPSC-EXOs and LPS-hDPSC-EXOs groups. The LPS-hDPSC-EXOs group exhibited the greatest tube structure and had the largest quantity in junction points and total tube lenght ($P < 0.05$; Fig. 4D-F). In addition, the expression of proangiogenic mRNA and antiangiogenic mRNA was estimated. Compared with those in the hDPSC-EXOs stimulation group, the VEGF and KDR mRNA levels were upregulated and the THBS mRNA levels were downregulated in the LPS-hDPSC-EXOs stimulation group ($P < 0.05$; Fig. 4G, H). However, compared to that in the control group, Ang-1 expression was decreased in the hDPSC-EXOs stimulation group and was not significantly changed in the LPS-hDPSC-EXOs stimulation group ($P > 0.05$; Fig. 4G). The results indicated that LPS-hDPSC-EXOs displayed better angiogenesis function than hDPSC-EXOs.

4. Differentially expressed exosomal microRNAs in hDPSC-EXOs and LPS-hDPSC-EXOs

To elucidate the different microRNA constituents of hDPSC-EXOs and LPS-hDPSC-EXOs, microRNA sequencing was conducted. The expression of 10 microRNAs was significantly up/downregulated in the LPS-hDPSC-EXOs, and of these microRNAs, 7 microRNAs (miR-146a-5p, miR-92b-5p, miR-218-5p, miR-23b-5p, miR-2110, miR-27a-5p, and miR-200b-3p) were upregulated and 3 microRNAs (miR-223-3p, miR-1246 and miR-494-3p) were downregulated (Fig. 5A, B). qRT-PCR analysis was used to verify the accuracy of the sequencing results. Consistent with the sequencing results, the expression of miR-146a-5p, miR-2110, and miR-200b-3p was upregulated in the LPS-hDPSC-EXOs, while the expression of miR-223-3p, miR-1246, and miR-494-3p was downregulated (Fig. 5C).

5. Pathway and GO analysis of genes targeted by differentially expressed microRNAs

The target genes of 10 differentially expressed microRNAs were predicted by 2 bioinformatics tools (miRanda and RNAhybrid). The intersection of the target gene was used for further GO and KEGG analysis.

GO analysis of the target genes showed the most significant biological processes, including cellular component organization, regulation of cellular communication, and cellular development process (Fig. 6A). KEGG pathway analysis showed that the targeted genes were involved in multiple important signal transductions (Fig. 6B), including the hypoxia inducible factor-1 (HIF-1) signaling pathway (Fig. 6C), Thyroid cancer related to angiogenesis, the Toll-like receptor signaling pathway (Fig. 6D), Bacterial invasion of epithelial cells related to inflammation, and Endocytosis related to exosome uptake.

Four different online microRNA databases (TargetScan, miRTarBase, miRDB, and miRWalk) were used to filter the angiogenesis-related genes targeted by the differentially expressed microRNAs. Genes that were indicated as targets by at least 2 of the databases mentioned above were included. Genes were annotated by the DAVID Bioinformatic database (https://david.ncifcrf.gov/). According to the GO term analysis, the genes that were related to the biological process of angiogenesis are shown in the mRNA-microRNA network (Fig. 7).

Discussion

Angiogenesis is a prerequisite for and hallmark of dental pulp repair and regeneration[17]. Neovascularization allows regenerative pulp tissue to perform its physiological function by providing oxygen, delivering nutrients and facilitating immune response. hDPSCs are regarded as reliable candidates for stem cell-based regeneration strategies due to their outstanding proangiogenic abilities[18]. The proangiogenic effect of hDPSCs has been proven in vivo and in vitro[19, 20]. However, whether hDPSCs display different proangiogenic abilities in an inflammatory microenvironment remains largely unknown. In a previous study, increased blood vessel density was detected in dental pulp extracted from deep caries[19, 20]. This result indicates that angiogenesis may also take place in response to inflammation[22, 23]. In another study, the vascular network formation of HUVECs was significantly enhanced in a coculture system of hDPSCs and HUVECs with the addition of TNF-α[24]. In our research, when stimulated with 5 μg/ml LPS, the hDPSCs displayed stronger angiogenesis-promoting effects on HUVECs than the normal control hDPSCs. Our finding is consistent with the studies mentioned above. We hypothesize that in the early stage of inflammation, hDPSCs may play a protective role in tissue repair by reacting to inflammatory factors and then promote angiogenesis in HUVECs. Further studies are needed to demonstrate how hDPSCs respond to different types of inflammatory factors.

hDPSCs could regulate the function of HUVECs through various kinds of intercellular communication, such as paracrine and juxtacrine communication[25]. As an important component of paracrine,

exosomes carry specific biomolecules, including proteins, mRNAs, and microRNAs. It has been widely reported that exosomes play an important role in regulating multiple regeneration processes[26, 27]. In a study by Xian et al., exosomes derived from hDPSCs were shown to promote the angiogenic potential of HUVECs by inhibiting the p38 MAPK signaling pathway[5]. Under inflammatory conditions, exosomes seem to have different capabilities. In another study, when cocultured with exosomes derived from LPS-pretreated hDPSCs, Schwann cells showed better migration and odontoblast differentiation abilities[28]. Furthermore, EVs from periodontitis-hDPSCs exhibited a stronger effect on angiogenesis and wound healing[13]. In our study, we demonstrated that the stronger proangiogenic paracrine activity of inflammation-induced hDPSCs was mediated by exosomes. We also observed that the release of exosomes enhanced with increased LPS concentration. Our study provides strong evidence that exosomes are crucial for stem cell-based regeneration.

The cell signaling pathways by which hDPSC-EXOs regulate angiogenesis in an inflammatory environment remain unclear. Exosomal microRNAs negatively regulate the expression of their target genes by binding to the 3'UTRs of the target genes, causing translational repression[29, 30]. By conducting microRNA sequencing, we found that the expression of certain microRNAs was downregulated/upregulated in the LPS-hDPSC-EXOs. In total, the expression of 10 microRNAs was significantly altered in response to LPS stimulation in our study, and of these microRNAs, 7 microRNAs were increased (miR-146a-5p, miR-92b-5p, miR-218-5p, miR-23b-5p, miR-2110, miR-27a-5p, and miR-200b-3p) and 3 microRNAs were decreased (miR-223-3p, miR-1246 and miR-494-3p). Among microRNAs, 5 microRNAs have been proven to play important roles in inflammation and HUVEC function and angiogenesis. We assume that the differentially expressed exosomal microRNAs might be the reason why inflammation-stimulated hDPSCs display a stronger revascularization role.

MiR-223-3p has been confirmed to regulate the function of various systems, including the cardiovascular system and immune system[31]. In head and neck squamous cell carcinoma (HNSCC) tissues, miR-223-3p expression was negatively correlated with CD31 expression, indicating its antiangiogenic properties[32]. The mRNA and protein expression of VEGF was significantly increased in breast cancer cells in which miR-223-3p was inhibited in vitro[33]. Furthermore, miR-223 was deregulated in several types of inflammatory diseases, such as sepsis, type 2 diabetes, and rheumatoid arthritis[34]. Taken together, these findings suggest that miR-223-3p is a strong candidate for the mechanism by which LPS-hDPSC-EXO-derived microRNA promotes the angiogenesis of HUVECs. We also found some other interesting observation by reviewing articles. In the study by Li et al., the expression of miR-146a was induced by LPS treatment. Angiogenesis was inhibited by miR-146a knockdown via TGF-β1 signaling pathway activation[35]. In another study, the expression level of miR-218-5p in glomerular mesangial cells (GMCs) was upregulated by LPS stimulation[36]. MiR-218-5p knockdown promoted the apoptosis of HUVECs by activating HMGB1[37]. MiR-200b-3p was reported to affect HUVEC functions by directly regulating a variety of proangiogenic genes (e.g., VEGFA) and anti-angiogenic target genes (e.g., KLF2)[38]. A previous study revealed that miR-1246 inhibited angiogenesis by repressing NF-κB signaling[39]. Further studies are required to demonstrate how certain LPS-hDPSC-EXOs microRNAs promote the angiogenesis of HUVECs.

Conclusion

In the current study, we found that LPS-hDPSC-EXOs displayed a stronger effect on promoting the angiogenesis of HUVECs than hDPSC-EXOs. Our study also showed that the altered expression of certain exosomal microRNAs might be the reason for the enhanced proangiogenic ability of LPS-stimulated hDPSCs. To the best of our knowledge, this is the first study to demonstrate the role of exosomal microRNAs from hDPSCs in the inflammation-induced angiogenesis. The current study may shed light on the effect of inflammation-stimulated hDPSCs on tissue regeneration.

Abbreviations

hPDSCs
Human dental pulp stem cells; **HUVECs**:Human Umbilical Vein Endothelial Cells; **MSC**:Mesenchymal stem cell; **LPS**:Lipopolysaccharides; **EVs**:Extracellular vesicles; **hDPSC-EXOs**:Exosomes derived from hDPSCs; **LPS-hDPSC-EXOs**:Exosomes derived from LPS-stimulated hDPSCs; **FBS**:Fetal bovine serum:**DMEM**:Dulbecco's modified eagle's medium; **PBS**:Phosphate-buffered saline; **EGM-2**:Endothelial growth medium-2; **CCK-8**:Cell counting kit-8; **TEM**:Transmission electron microscopy; **NTA**:Nanoparticle tracking assay; **DAPI**:4',6-diamidino-2-phenylindole; **qRT-PCR**:Quantitative reverse-transcription polymerase chain reaction; **HSP70**:Heat shock protein 70; **VEGF**:Vascular endothelial growth factor; **KDR**:Kinase-insert domain-containing receptor; **Ang-1**:Angiopoietin 1; **THBS**:Thrombospondin 1; **IL-6**:Interleukin-6; **TNF-α**:Tumor necrosis factor alpha; **GAPDH**:Glyceraldehyde-3-phosphate dehydrogenase; **GO**:Gene Ontology; **KEGG**:Kyoto Encyclopedia of Genes and Genomes; **BP**:Biological processes; **CC**:Cellular components; **M**F:Molecular functions; **MAPK**:Mitogen-activated protein kinase; **HIF-1**:Hypoxia inducible factor-1; **HNSCC**:Head and neck squamous cell carcinoma; **GMCs**:Glomerular mesangial cells

Declarations

Acknowledgements

Not applicable.

Authors' contributions

XWA and WBL contributed to the conception and logic of the article. HXY and QW contributed to the writing and drafting of the manuscript. HXY, PYH, LJJ, CZ, ZKY and LYF performed the experiments, collection of data, data analysis, and interpretation. XWA, WBL, and QW contributed to the critical revision of the manuscript for important intellectual content; all the authors have given final approval of the version to be published and agree to be accountable for all aspects of the work.

Funding

This study was supported by the National Natural Science Foundation of China (81870755, 81700956).

Availability of data and materials

The data supporting the research results obtained from the corresponding authors according to reasonable requirements.

Ethics approval and consent to participate

This study was approved by the Ethics Committee of Nanfang Hospital, Southern Medical University. Written informed consent was obtained from all adult patients.

Consent for publication

Not applicable.

Competing interests

The authors declare that they have no competing interests.

References

1. Ratajczak J, Bronckaers A, Dillen Y, Gervois P, Vangansewinkel T, Driesen RB, et al. The Neurovascular Properties of Dental Stem Cells and Their Importance in Dental Tissue Engineering. Stem Cells Int. 2016;2016:9762871.
2. Rombouts C, Giraud T, Jeanneau C, About I. Pulp Vascularization during Tooth Development, Regeneration, and Therapy. J Dent Res. 2017;96:137-44.
3. Lambrichts I, Driesen RB, Dillen Y, Gervois P, Ratajczak J, Vangansewinkel T, et al. Dental Pulp Stem Cells: Their Potential in Reinnervation and Angiogenesis by Using Scaffolds. J Endod. 2017;43:S12-6.
4. Rombouts C, Giraud T, Jeanneau C, About I. Pulp Vascularization during Tooth Development, Regeneration, and Therapy. J Dent Res. 2017;96:137-44.
5. Xian X, Gong Q, Li C, Guo B, Jiang H. Exosomes with Highly Angiogenic Potential for Possible Use in Pulp Regeneration. J Endod. 2018;44:751-8.
6. Fawzy EK, Elsalawy R, Ibrahim N, Gadalla M, Albargasy H, Zahra N, et al. The Dental Pulp Stem/Progenitor Cells-Mediated Inflammatory-Regenerative Axis. Tissue Eng Part B Rev. 2019;25:445-60.
7. Soden RI, Botero TM, Hanks CT, Nor JE. Angiogenic signaling triggered by cariogenic bacteria in pulp cells. J Dent Res. 2009;88:835-40.
8. Botero TM, Son JS, Vodopyanov D, Hasegawa M, Shelburne CE, Nor JE. MAPK signaling is required for LPS-induced VEGF in pulp stem cells. J Dent Res. 2010;89:264-9.
9. Pittenger MF, Le Blanc K, Phinney DG, Chan JK. MSCs: Scientific Support for Multiple Therapies. Stem Cells Int. 2015;2015:280572.

10. Huang L, Ma W, Ma Y, Feng D, Chen H, Cai B. Exosomes in mesenchymal stem cells, a new therapeutic strategy for cardiovascular diseases? Int J Biol Sci. 2015;11:238-45.
11. Phinney DG, Pittenger MF. Concise Review: MSC-Derived Exosomes for Cell-Free Therapy. Stem Cells. 2017;35:851-8.
12. Zhou Y, Xu H, Xu W, Wang B, Wu H, Tao Y, et al. Exosomes released by human umbilical cord mesenchymal stem cells protect against cisplatin-induced renal oxidative stress and apoptosis in vivo and in vitro. Stem Cell Res Ther. 2013;4:34.
13. Zhou H, Li X, Yin Y, He XT, An Y, Tian BM, et al. The proangiogenic effects of extracellular vesicles secreted by dental pulp stem cells derived from periodontally compromised teeth. Stem Cell Res Ther. 2020;11:110.
14. Kong Y, Hu X, Zhong Y, Xu K, Wu B, Zheng J. Magnesium-enriched microenvironment promotes odontogenic differentiation in human dental pulp stem cells by activating ERK/BMP2/Smads signaling. Stem Cell Res Ther. 2019;10:378.
15. Ma D, Yu H, Xu S, Wang H, Zhang X, Ning T, et al. Stathmin inhibits proliferation and differentiation of dental pulp stem cells via sonic hedgehog/Gli. J Cell Mol Med. 2018;22:3442-51.
16. Witwer KW, Buzas EI, Bemis LT, Bora A, Lasser C, Lotvall J, et al. Standardization of sample collection, isolation and analysis methods in extracellular vesicle research. J Extracell Vesicles. 2013;2.
17. Griffioen AW, Molema G. Angiogenesis: potentials for pharmacologic intervention in the treatment of cancer, cardiovascular diseases, and chronic inflammation. Pharmacol Rev. 2000;52:237-68.
18. Nakashima M, Iohara K, Sugiyama M. Human dental pulp stem cells with highly angiogenic and neurogenic potential for possible use in pulp regeneration. Cytokine Growth Factor Rev. 2009;20:435-40.
19. Iohara K, Zheng L, Wake H, Ito M, Nabekura J, Wakita H, et al. A novel stem cell source for vasculogenesis in ischemia: subfraction of side population cells from dental pulp. Stem Cells. 2008;26:2408-18.
20. Nakashima M, Iohara K, Sugiyama M. Human dental pulp stem cells with highly angiogenic and neurogenic potential for possible use in pulp regeneration. Cytokine Growth Factor Rev. 2009;20:435-40.
21. Soden RI, Botero TM, Hanks CT, Nor JE. Angiogenic signaling triggered by cariogenic bacteria in pulp cells. J Dent Res. 2009;88:835-40.
22. Carmeliet P. Mechanisms of angiogenesis and arteriogenesis. Nat Med. 2000;6:389-95.
23. Semenza GL. Vasculogenesis, angiogenesis, and arteriogenesis: mechanisms of blood vessel formation and remodeling. J Cell Biochem. 2007;102:840-7.
24. An L, Shen S, Wang L, Li Y, Fahim S, Niu Y, et al. TNF-alpha increases angiogenic potential in a co-culture system of dental pulp cells and endothelial cells. Braz Oral Res. 2019;33:e59.

25. Gong T, Xu J, Heng B, Qiu S, Yi B, Han Y, et al. EphrinB2/EphB4 Signaling Regulates DPSCs to Induce Sprouting Angiogenesis of Endothelial Cells. J Dent Res. 2019;98:803-12.
26. Fan J, Wei Q, Koay EJ, Liu Y, Ning B, Bernard PW, et al. Chemoresistance Transmission via Exosome-Mediated EphA2 Transfer in Pancreatic Cancer. Theranostics. 2018;8:5986-94.
27. Phinney DG, Pittenger MF. Concise Review: MSC-Derived Exosomes for Cell-Free Therapy. Stem Cells. 2017;35:851-8.
28. Li J, Ju Y, Liu S, Fu Y, Zhao S. Exosomes derived from lipopolysaccharide-preconditioned human dental pulp stem cells regulate Schwann cell migration and differentiation. Connect Tissue Res. 2019:1-10.
29. Liang X, Zhang L, Wang S, Han Q, Zhao RC. Exosomes secreted by mesenchymal stem cells promote endothelial cell angiogenesis by transferring miR-125a. J Cell Sci. 2016;129:2182-9.
30. Hu X, Zhong Y, Kong Y, Chen Y, Feng J, Zheng J. Lineage-specific exosomes promote the odontogenic differentiation of human dental pulp stem cells (DPSCs) through TGFbeta1/smads signaling pathway via transfer of microRNAs. Stem Cell Res Ther. 2019;10:170.
31. Han J, Zhao F, Zhang J, Zhu H, Ma H, Li X, et al. miR-223 reverses the resistance of EGFR-TKIs through IGF1R/PI3K/Akt signaling pathway. Int J Oncol. 2016;48:1855-67.
32. Bozec A, Zangari J, Butori-Pepino M, Ilie M, Lalvee S, Juhel T, et al. MiR-223-3p inhibits angiogenesis and promotes resistance to cetuximab in head and neck squamous cell carcinoma. Oncotarget. 2017;8:57174-86.
33. Wang X, Tong Z, Liu H. MiR-223-3p targeting epithelial cell transforming sequence 2 oncogene inhibits the activity, apoptosis, invasion and migration of MDA-MB-468 breast cancer cells. Onco Targets Ther. 2019;12:7675-84.
34. Aziz F. The emerging role of miR-223 as novel potential diagnostic and therapeutic target for inflammatory disorders. Cell Immunol. 2016;303:1-6.
35. Li Y, Zhu H, Wei X, Li H, Yu Z, Zhang H, et al. LPS induces HUVEC angiogenesis in vitro through miR-146a-mediated TGF-beta1 inhibition. Am J Transl Res. 2017;9:591-600.
36. Zhang T, Xiang L. Honokiol alleviates sepsis-induced acute kidney injury in mice by targeting the miR-218-5p/heme oxygenase-1 signaling pathway. Cell Mol Biol Lett. 2019;24:15.
37. Yu SF, Feng WY, Chai SQ, Meng XB, Dou ZX, Zhu H. Down-Regulation of miR-218-5p Promotes Apoptosis of Human Umbilical Vein Endothelial Cells Through Regulating High-Mobility Group Box-1 in Henoch-Schonlein Purpura. Am J Med Sci. 2018;356:64-71.
38. Bartoszewski R, Serocki M, Janaszak-Jasiecka A, Bartoszewska S, Kochan-Jamrozy K, Piotrowski A, et al. miR-200b downregulates Kruppel Like Factor 2 (KLF2) during acute hypoxia in human endothelial cells. Eur J Cell Biol. 2017;96:758-66.
39. Bai Y, Wang W, Sun G, Zhang M, Dong J. Curcumin inhibits angiogenesis by up-regulation of microRNA-1275 and microRNA-1246: a promising therapy for treatment of corneal neovascularization. Cell Prolif. 2016;49:751-62.

Figures

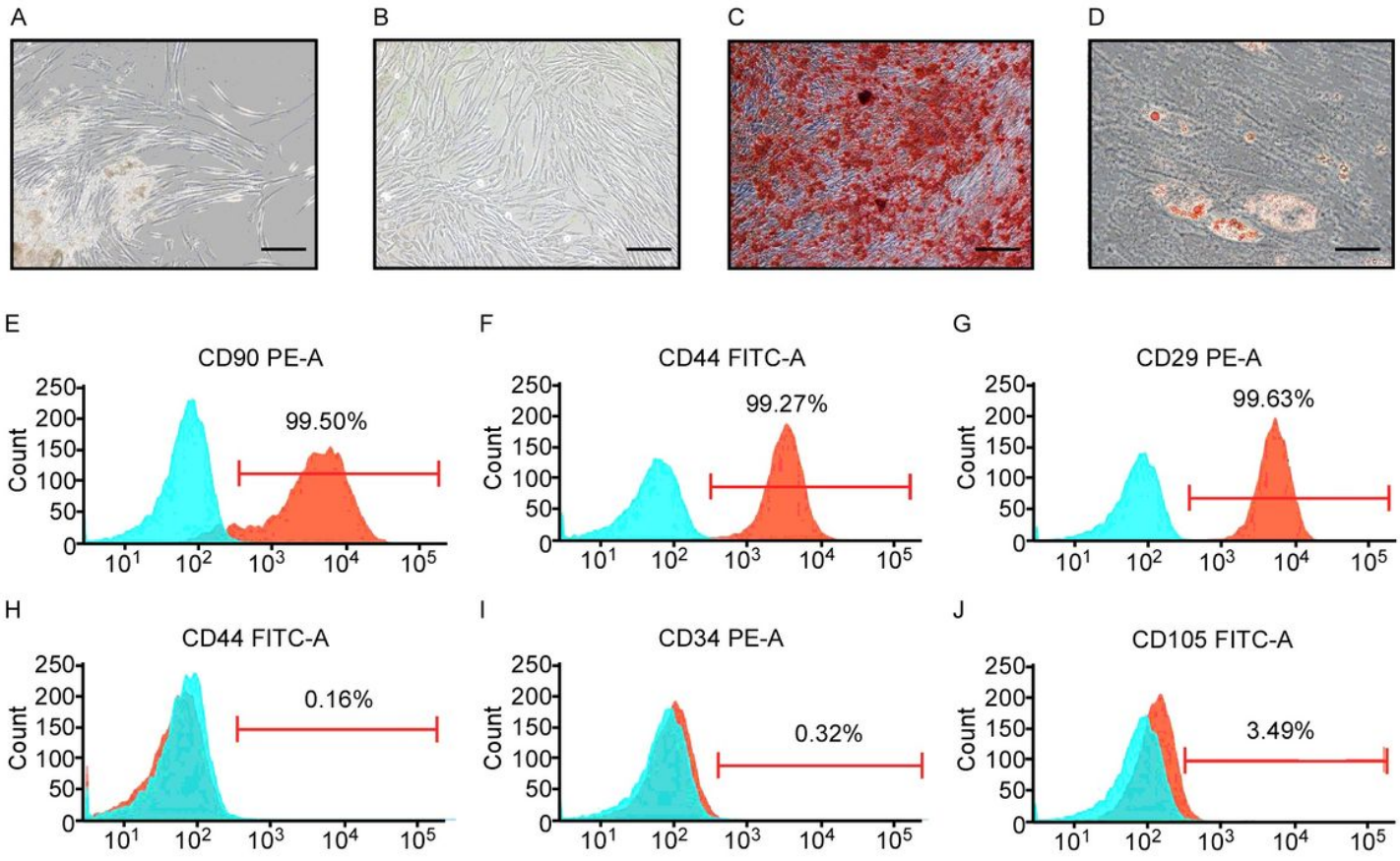

Figure 1

Isolation and identification of hDPSCs. (A) Primary cultured hDPSCs (scale bar, 200 μm). (B) The cell morphology of hDPSCs was observed under an optical microscope (scale bar, 200 μm). (C) Osteogenic differentiation assay of hDPSCs (scale bar, 200 μm). (D) Adipogenic differentiation assay of hDPSCs (scale bar, 50 μm). (E-J) Flow cytometry assays showed high levels of the mesenchymal stem cell markers CD90 (90.50%), CD44 (99.27%), and CD29 (99.63%) and low levels of the hematopoietic cell markers CD45 (0.16%), CD34 (0.32%), and CD105 (3.49%) in hDPSCs.

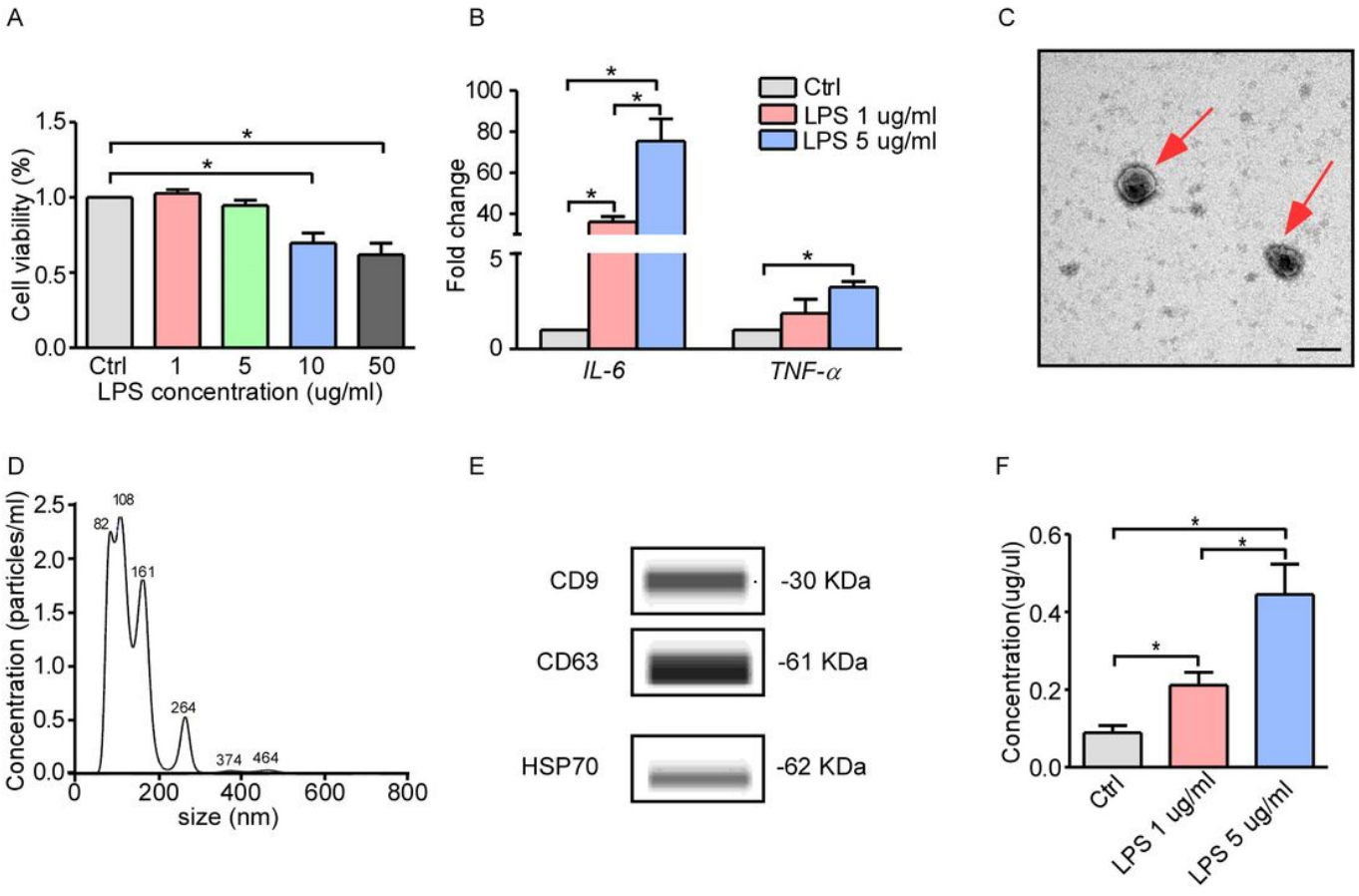

Figure 2

Extraction of exosomes derived from LPS-stimulated hDPSCs. (A) hDPSCs were treated with different concentrations of LPS for 2 days; cell viability was detected by the CCK-8 assay. (B) The IL-6 and TNF-α mRNA expression in LPS-stimulated hDPSCs was detected by qRT-PCR. (C) TEM showed the classic morphology of hDPSC-EXOs, which resembled a cup and saucer and had a bilayer membrane (scale bar, 200 nm). (D) The size of the EVs was detected by NTA. (E) The expression of the exosomal surface markers CD9, CD63, and HSP70 were detected by Western blotting. (F) The volume of exosomes secreted from hDPSCs treated with different concentrations of LPS was detected by BCA assay. Data represent means ± SD. *P < 0.05.

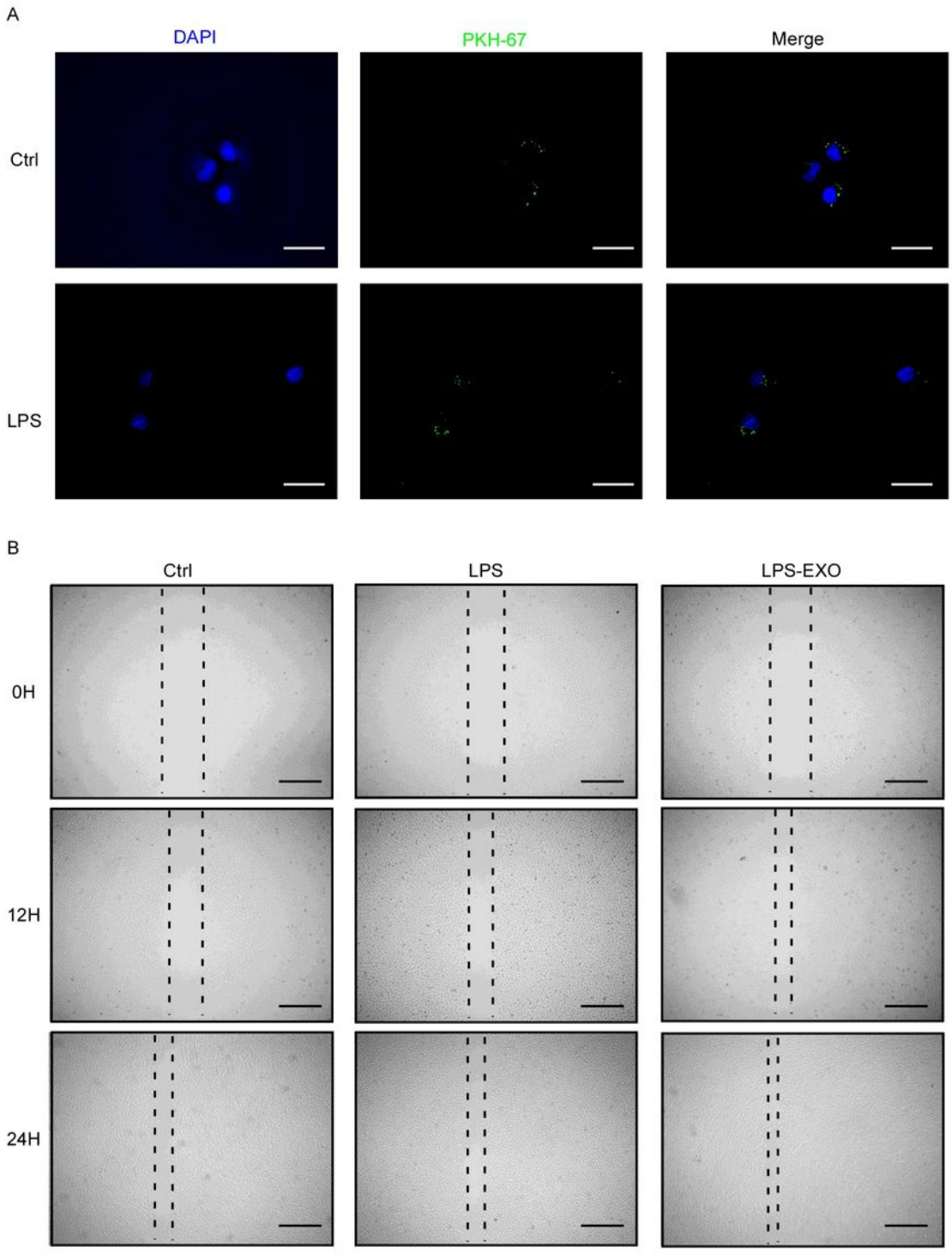

Figure 3

The migration of HUVECs was promoted by endocytosis of LPS-DPSC-EXOs. (A) Endocytosis of PKH-67-labeled exosomes by HUVECs (scale bar, 50 μm). (B) Scratch wound-healing assay. LPS-DPSC-EXOs promote the migration of HUVECs (scale bar, 200 μm).

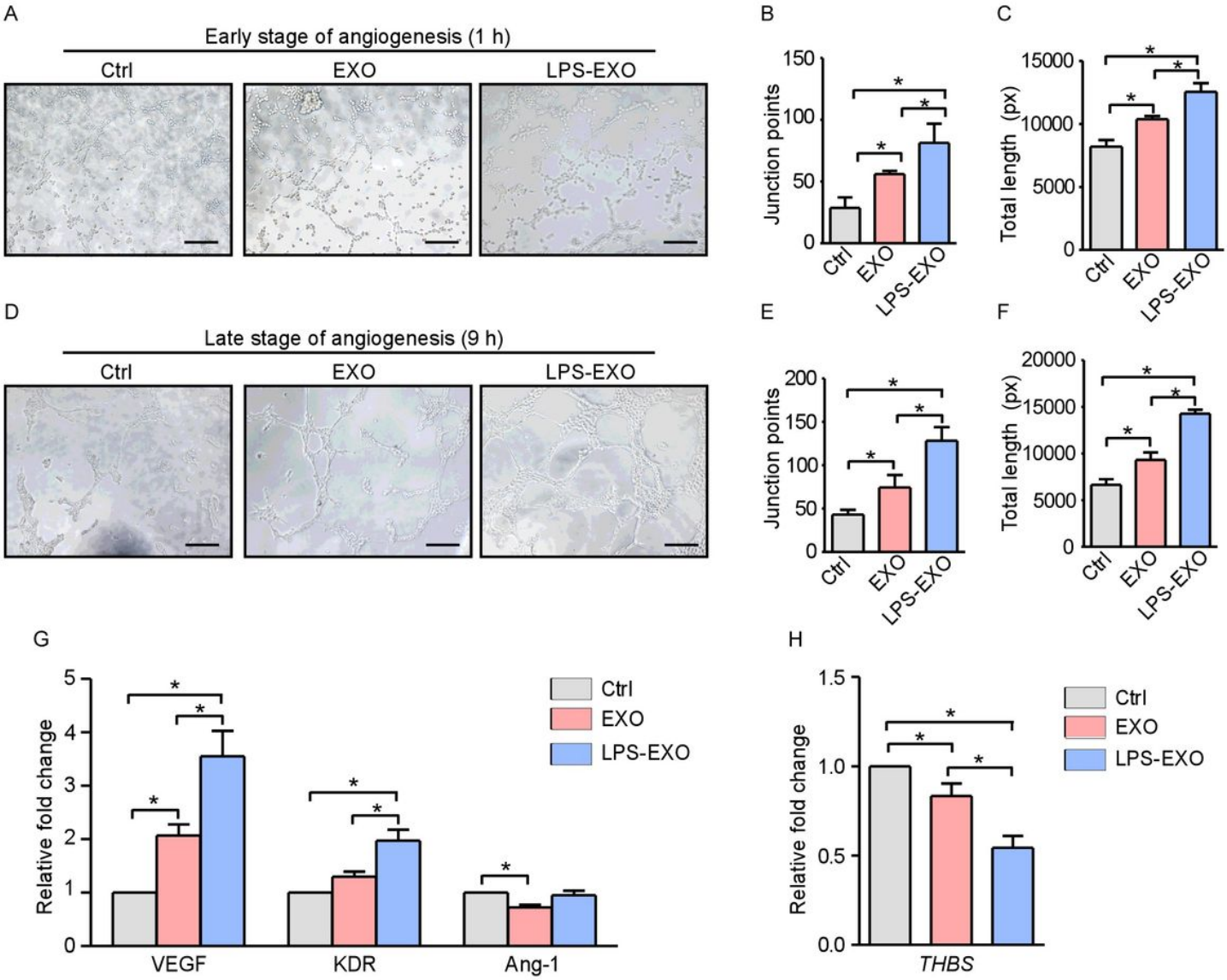

Figure 4

LPS-DPSC-EXOs promote the angiogenesis of HUVECs. (A) Representative images of the tube formation assay at 1 hours (scale bar, 200 μm). (B-C) Quantification analysis of the number of junction points (B), total length (C) at 1 hours. (D) Representative images of the tube formation assay at 9 hours (scale bar, 200 μm). (E-F) Quantification analysis of the number of junction points (D), total length (E) at 9 hours. (G) The mRNA expression of proangiogenic genes (VEGF, KDR, and Ang-1). (H) The mRNA expression of antiangiogenic genes (THBS). Data represent means ± SD. *P < 0.05.

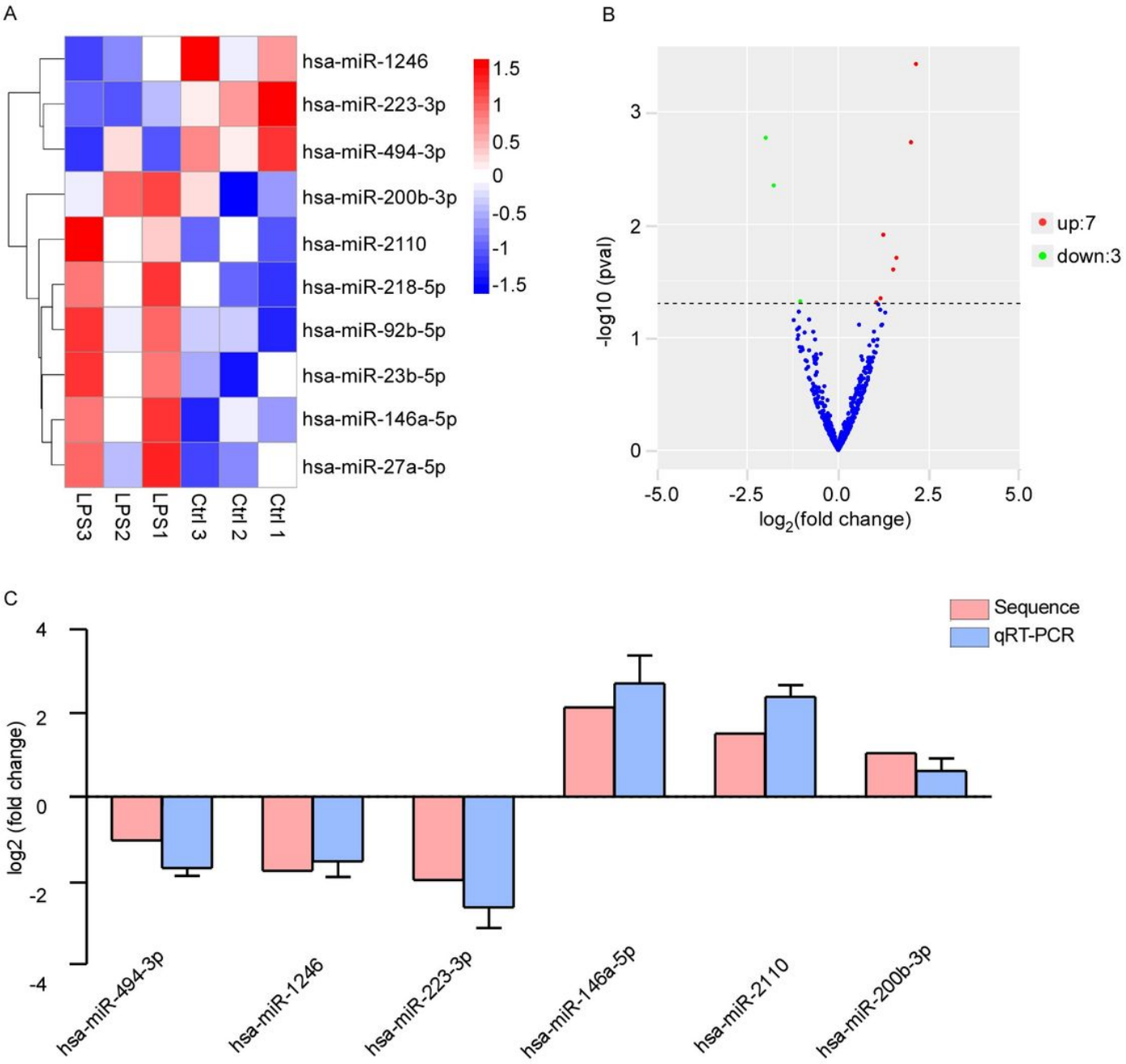

Figure 5

MicroRNA sequencing of hDPSC-EXOs and LPS-hDPSC-EXOs. (A) Heat map and cluster analysis show that the expression of 10 microRNAs was significantly changed in LPS-hDPSC-EXOs, and of these microRNAs, 7 were increased and 3 were decreased. (B) MicroRNA volcano plot. (C) Comparison of microRNA sequencing and qRT-PCR data. Data represent means ± SD.

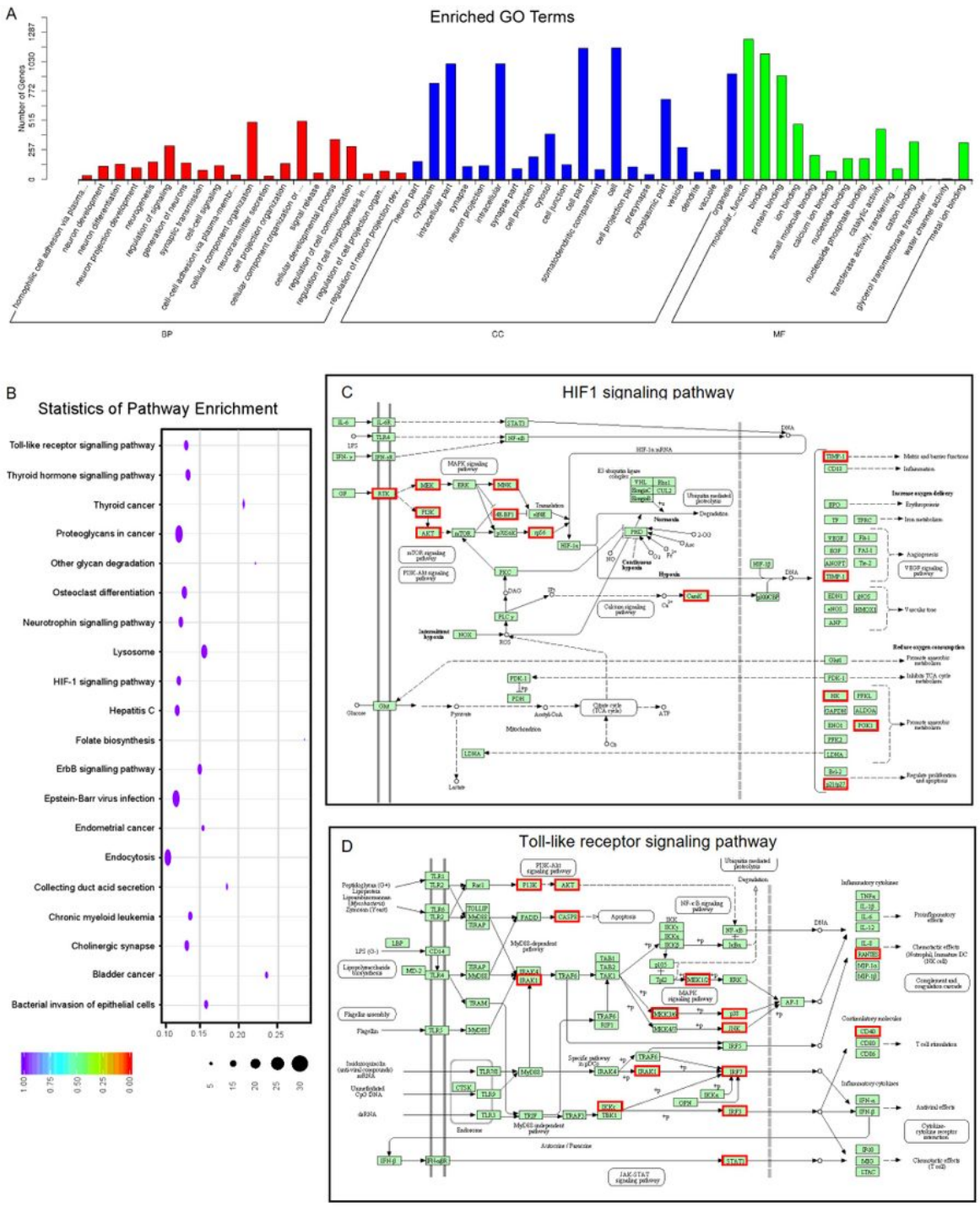

Figure 6

GO annotation and KEGG pathway analysis of differentially expressed microRNAs. (A) GO enrichment analysis of genes targeted by differentially expressed microRNAs. (B) KEGG pathway analysis of differentially expressed microRNAs. (C) HIF-1 signaling pathway map. (D) Toll-like receptor signaling pathway map. Target genes of differentially expressed microRNAs are marked in red.

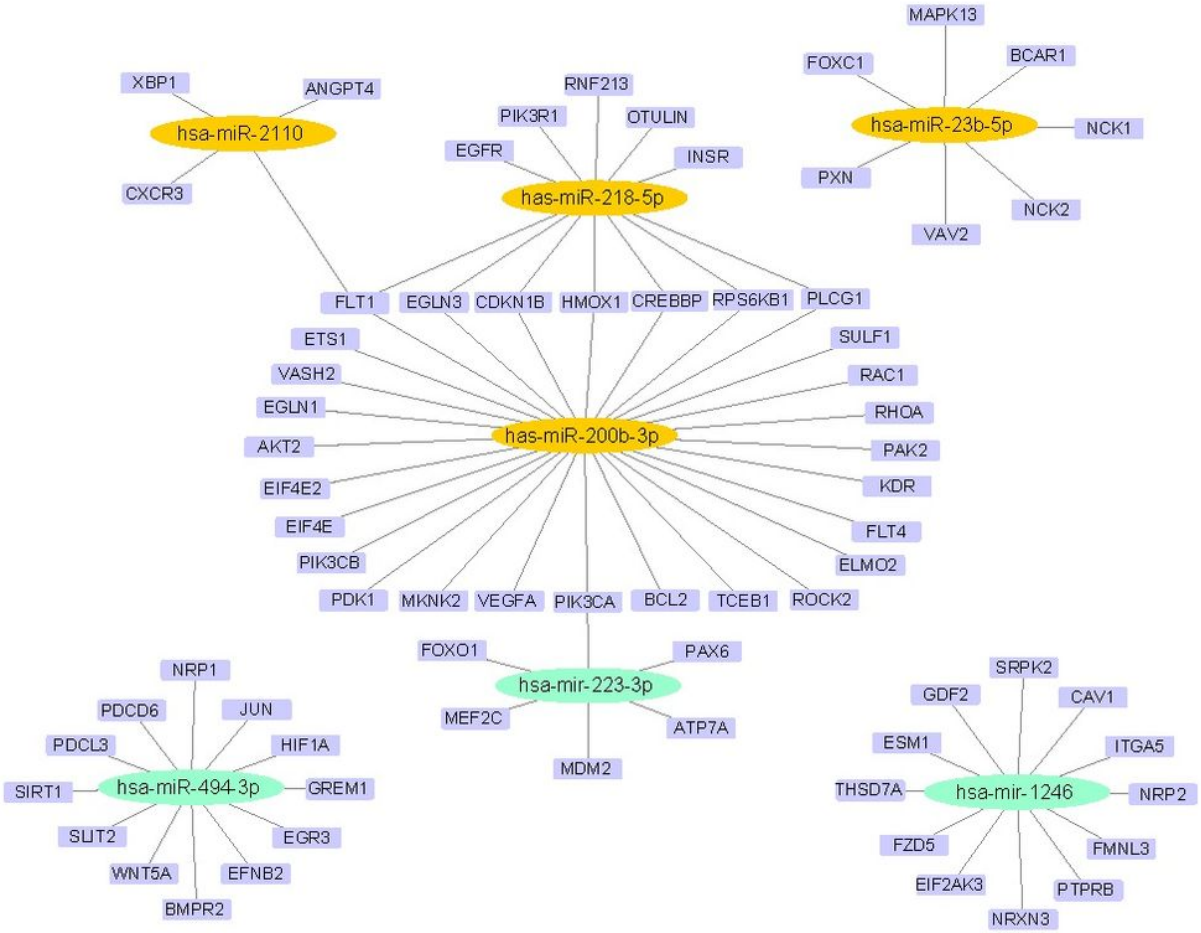

Figure 7

The regulatory networks of microRNAs and angiogenesis-related target genes.